

ON SOME OPTIMAL MIMO ANTENNA COEFFICIENTS IN MULTIPATH CHANNELS

A. Alayón Glazunov^{1,*} and J. Zhang²

¹Division of Electromagnetic Engineering, School of Electrical Engineering, KTH Royal Institute of Technology, Teknikringen 33, SE-100 44 Stockholm, Sweden

²Communications Group, Department of Electronic and Electrical Engineering, University of Sheffield, Mappin Street, Sheffield, S1 3JD, UK

Abstract—This paper derives some optimum transmit and receive antenna coefficients in wireless multipath channels based on the spherical vector wave multimode expansion of the multiple-input multiple-output (MIMO) channel matrix. The derived antenna coefficients satisfy the following specific optimization criteria: (i) maximum MIMO mean effective link gain (link MEG) based on the multimode channel realizations or (ii) maximum MIMO link MEG based on the multimode correlation matrix or (iii) correlation minimization by diagonalization of the MIMO full-correlation matrix. It is shown that the proposed approach leads to matrix equations belonging to the nearest Kronecker product (NKP) problem family, which in general have no trivial solution. However, we show that exact solutions are provided to the posed NKP problems under the assumption of the Kronecker model for the MIMO full-correlation matrix. The results are illustrated by numerical examples. The proposed approach is a complement to existing antenna pattern analysis methods.

1. INTRODUCTION

It is well-known that two parameters have a fundamental impact on the spectral efficiency and channel capacity of Multiple-Input Multiple-Output (MIMO) links over multipath wireless channels: i) the signal-to-noise ratio (SNR) and ii) the correlation statistics of

Received 23 August 2011, Accepted 26 September 2011, Scheduled 13 October 2011

* Corresponding author: Andrés Alayón Glazunov (aag@ee.kth.se).

the MIMO channel matrix [1–4]. The SNR is directly proportional to the link gain, which is basically the mean effective gain (MEG) between a receive and a transmit antenna in multipath channels (Some authors use Mean Effective Link Gain (MELG), see [5]). Hence, maximizing MEG implies that SNR requirements can be met without increasing transmit power which in addition will improve battery life of handsets. Moreover, MEG maximization for MIMO systems is equivalent to beamforming, which depending on channel conditions, e.g., low angle spread, can give substantial system gain. MEG is used in the evaluation of the standardized communication performance measurements of handheld terminals [6]. The correlation characteristics are in turn given by the correlation matrix of the MIMO channel matrix (It is worthwhile to note that the diagonal elements of the correlation matrix contain the MEG for each transmit-receive antenna pair.). Diversity gain and multiplexing gain are both achieved by processing uncorrelated channels. Hence, minimizing the correlation between the links may maximize these gains. The correlation and the link gain both depend on the properties of the channel and the antennas. Hence, an accurate characterization of the antenna-channel interactions is required for a practical implementation and evaluation of the performance of MIMO technologies in 4G and beyond wireless systems [6].

MIMO techniques, smart antenna techniques and diversity techniques have all been extensively studied for a variety of antenna configurations [7, 8]. However, the joint characterization of transmit and receive antenna systems has only recently been treated in a rigorous manner [9, 10]. In [11] the main focus has been on the characterization of mutual coupling of closely placed antenna elements. Many interesting approaches have been developed that circumvent the impairments caused by the mutual coupling of the antennas through clever matching network designs [12]. These prior studies have shown relevant findings concerning the effects of mutual coupling on MIMO system performance. Moreover, a few papers describe the optimal antenna coefficients for MIMO systems [13–15].

The goal of this paper is to add new insights to those findings on the basis of the interaction of the antennas with the channel and to extend upon previous results for the SIMO (Single-Input Multiple-Output) and MISO (Multiple-Input Single-Output) cases within the spherical vector wave framework [16]. Our starting point is the formalism developed in [16–18] for the joint characterization of antenna systems and propagation channels that uses the antenna scattering matrix [19] and the spherical vector wave (svw) expansion of the electromagnetic fields [20] as the two main tools. Our characterization

is applicable to arbitrary MIMO antennas in arbitrary electromagnetic fields; it naturally expresses the polarization, the angle, and the spatial diversity inherent to MIMO systems encompassing both antennas and channels within the same framework. Moreover, this expansion gives a condensed interpretation of the radiation properties of an antenna. In [17] we expanded the MIMO channel matrix \mathbf{H} into spherical vector wave modes \mathbf{M} , which is general except for the assumption that both transmit and receive antennas are in each others' far-field region. A method for computing the mutual impedance that relies on the svw multipole expansion of the fields is found in [21]. Together, these tools provide a straightforward and insightful way into antenna design and performance characterization of antennas.

The contributions of this paper are summarized as follows:

- We provide a novel definition of the Mean Effective Gain (MEG) of multi-element antennas over a multipath MIMO wireless link. This definition is expressed in terms of the multimode expansion coefficients of the MIMO channel matrix. This definition provides straightforward information about which modes should be excited by the antennas at both ends of a MIMO link.
- We show that if the multimode expansion coefficients of the MIMO channel are known, then the maximum link power, and hence the MEG too, is achieved by a joint conjugate multimode matching of the receive and transmit antenna coefficients. In this case the MIMO system performance is maximized for channels with low angle spread through beamforming applied to the svw modes.
- We further show that if the correlation matrix multimode expansion coefficients of the MIMO channel is known, then the maximum link power/MEG is achieved over the link corresponding to the strongest eigenmode of the multimode correlation matrix. Also here, the receive and transmit antenna coefficients are jointly optimized.
- We also show that independent MIMO channels are achieved by the joint transmission and reception over the strongest eigenmodes of the multimode correlation matrix, i.e., a diagonalization of the correlation matrix is obtained. In this case the transmission rate of a MIMO system is maximized.
- Based on the above results we provide bounds for the MEG in the MIMO case for three cases: (i) maximum MIMO mean effective link gain (link MEG) based on the multimode channel realizations or (ii) maximum MIMO link MEG based on the multimode correlation matrix or (iii) correlation minimization by diagonalization of the MIMO full-correlation matrix.

- We show that the joint optimization of the receive and transmit MIMO coefficients belongs to the family of nearest Kronecker product (NKP) problems. While a general solution to this problem does not exist, we find exact solutions under the assumption of the Kronecker model for the correlation matrix.

2. MULTIMODE REPRESENTATION ANTENNAS AND CHANNELS

2.1. Mode-to-mode MIMO Channel Matrix \mathbf{M}

Consider two multiport antennas separated by a distance d from each other, such that a) there is no mutual coupling between the Tx and Rx antennas and b) there is no coupling to nearby scatterers. However, coupling between antenna elements at Rx or Tx is allowed. We further assume that each antenna phase center coincides with the origin of their own coordinate system. Assume now that the receive and the transmit multi-element antenna system are enclosed by an imaginary sphere of radius a_r and a_t as shown in Figure 1. It has been shown in [19] that the electric field outside this sphere can be expanded in *spherical vector wave modes*. This field representation allows a joint characterization of the receive and transmit antennas and the propagation channel of any communication system. It has been shown in [16,17] that the *scattering matrix* description of the antennas [17, 19] provides the

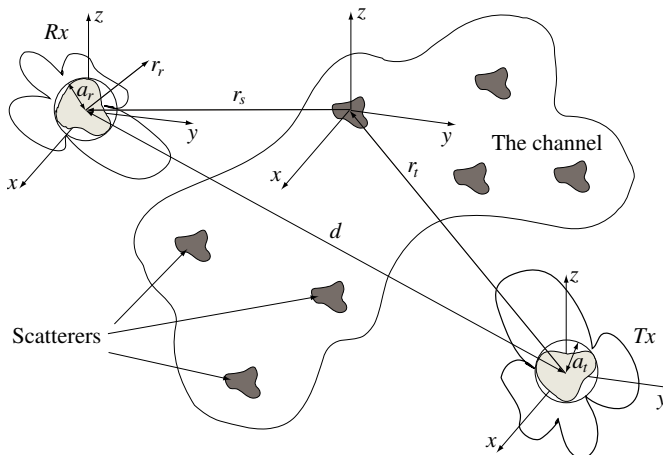


Figure 1. Schematic representation of the propagation channel with non interacting scatterers and the antennas.

following (noise-free) input-output relationship for a MIMO link

$$\mathbf{w} = \mathbf{RMT}\mathbf{v}, \quad (1)$$

where the MIMO channel transfer function is expressed as

$$\mathbf{H} = \mathbf{RMT}, \quad (2)$$

where at the transmit antenna side, we have $\mathbf{v} \in \mathbb{C}^{N_t \times 1}$, which are the transmitted (According to the multiport network definitions these are the signals incoming at the local ports of the antenna, in this case the transmit antenna.) signals, $\mathbf{T} \in \mathbb{C}^{M_t \times N_t}$ is the matrix containing the coefficients of the transmit antenna, while at the receive antenna side $\mathbf{w} \in \mathbb{C}^{N_r \times 1}$ denotes the received signals (Again, following the multiport network definitions these are the signals outgoing from the local ports of the antenna, in this case the receive antenna.) and $\mathbf{R} \in \mathbb{C}^{N_r \times M_r}$ is the matrix containing the receive antenna coefficients. The mode-to-mode MIMO channel matrix, i.e., $\mathbf{M} \in \mathbb{C}^{M_r \times M_t}$ is either a random or a deterministic matrix that describes the properties of the wireless channel in terms of the multimode expansion coefficients of the electromagnetic field [17]. Also in [17] we provide the relationship between the statistics of the MIMO multimode channel expansion and the double-directional (DD) representation of the MIMO channel.

Another representation of (2) is given by

$$\mathbf{h} = (\mathbf{T}' \otimes \mathbf{R}) \mathbf{m}, \quad (3)$$

where $(\cdot)'$ denotes the matrix transpose operation, $\mathbf{h} = \text{vec}(\mathbf{H})$ and $\mathbf{m} = \text{vec}(\mathbf{M})$ are the vectorized forms of the \mathbf{H} -matrix and \mathbf{M} -matrix, respectively. Here the operator $\text{vec}(\mathbf{A}) = [\mathbf{A}'_1 \mathbf{A}'_2 \dots \mathbf{A}'_N]'$, where \mathbf{A}_j is the j column of matrix \mathbf{A} . The relationship of \mathbf{T} and \mathbf{R} to the far-field antenna pattern is given next.

2.2. Transmit \mathbf{T} and Receive \mathbf{R} Antenna Matrices

The elements of the transmission matrix $T_{\tau ml, n}$ are obtained as the projection of the far-field of the antenna on the spherical vector harmonics, $\mathbf{A}_{\tau ml}(\hat{\mathbf{r}})$. Hence, the far-field $\mathbf{F}_n(\hat{\mathbf{r}})$ of port n is given by

$$\mathbf{F}_n(\hat{\mathbf{r}}) = k\sqrt{2\eta} \sum_{l=1}^{\infty} \sum_{m=-l}^l \sum_{\tau=1}^2 i^{l+2-\tau} T_{\tau ml, n} \mathbf{A}_{\tau ml}(\hat{\mathbf{r}}) v_n, \quad (4)$$

where $\hat{\mathbf{r}}$ is the unitary spatial coordinate, η is the free-space impedance, k is the wave-number. To simplify the notation and manipulation of the variables we introduce the multi-index $\kappa \rightarrow (\tau, m, l)$, which is computed as $\kappa = 2(l^2 + l - 1 + m) + t$ for $l = 1 \dots l_{\max}$, $m = -l \dots l$ and $\tau = 1, 2$. We use the multi-index $\iota \rightarrow (t, \mu, \lambda)$ to denote svw expansion

coefficients at the other end of the communication link. The multipoles are classified as either TE ($\tau = 1$) or TM ($\tau = 2$). The azimuthal and radial dependencies are given by the m and l index, respectively. The imaginary unit is denoted by i .

For reciprocal antennas we have that

$$R_{n,\tau ml} = (-1)^m T_{\tau(-m)l,n}, \quad (5)$$

where $R_{n,\tau ml}$ and $T_{\tau ml,n}$ are elements of matrices \mathbf{R} and \mathbf{T} , respectively. In practice, matrices \mathbf{R} and \mathbf{T} can be obtained from measurements or from numerical models of the antennas.

3. ANTENNA COEFFICIENT OPTIMIZATION

In this section we show some optimality relationships for matrices \mathbf{R} and \mathbf{T} as a function of the mode-to-mode channel matrix \mathbf{M} . This is equivalent to optimize the far-field antenna patterns given we know the orthogonally polarized field components impinging at the receive and transmit antenna positions for reciprocal channels and antennas.

Following (3) we see that the “instantaneous” link power of a MIMO link is given by

$$\|\mathbf{h}\|^2 = \|(\mathbf{T}' \otimes \mathbf{R}) \mathbf{m}\|^2, \quad (6)$$

where $\|\cdot\|$ denotes the vector norm.

We can now define the mean effective gain (MEG), which quantifies the link power in multipath channels [22, 23]. In [16] we gave a definition of MEG of an antenna in terms of the spherical vector wave expansion. Here, we extend this result to comprise the link power between two antennas or in general between two multi-element antenna systems.

Definition 1: The Mean Effective Gain (MEG) of a MIMO link is defined as

$$G_e = \frac{\text{tr}\{\mathcal{R}_h\}}{\text{tr}\{\mathcal{R}_m\}}, \quad (7)$$

where tr denotes the matrix trace operation, $\text{tr}\{\mathcal{R}_h\}$ is the average link power, $\text{tr}\{\mathcal{R}_m\}$ is the average link power of the multimode channel. The matrices

$$\mathcal{R}_h = \langle \mathbf{h}\mathbf{h}^\dagger \rangle = (\mathbf{T}' \otimes \mathbf{R}) \mathcal{R}_m (\mathbf{T}' \otimes \mathbf{R})^\dagger, \quad (8)$$

and

$$\mathcal{R}_m = \langle \mathbf{m}\mathbf{m}^\dagger \rangle, \quad (9)$$

are the *full-correlation matrices* of \mathbf{H} and \mathbf{M} , respectively.

The above definition characterizes the communication link performance of two antennas as compared to two ideal multi-element isotropic antennas that pick up all the available multi-pole channel power, i.e., the total available link power. The advantages of this definition are manifold, e.g., it follows the original definition of MEG [22] and therefore takes into account the properties of both the antennas and the propagation channel. The MEG can be alternatively defined relative practical antennas too, which serve as reference antennas. For example, dipole antennas are commonly used as a reference due to their radiation pattern characteristics and high efficiency [6]. In this case the MEG of the antennas under test defined relative dipole antennas is computed as follows: $G_d = \text{tr}\{\mathcal{R}_h\}/\text{tr}\{\mathcal{R}_h^d\}$, where $\text{tr}\{\mathcal{R}_h^d\}$ is the MIMO link power measured with the reference antennas. Results presented in this paper are specialized to the MEG as defined by (7), i.e., we use the ideal isotropic radiator as the reference antenna.

3.1. MIMO Link Power/MEG Maximization

Based on Definition 1 we see that there are two criteria on which we can base our MEG optimization:

- (i) The multimode field realizations of the channel \mathbf{m} .
- (ii) The correlation matrix of the multimode field realizations of the channel \mathcal{R}_m .

Inspecting (6) and (8) suggests to perform the maximization of the MEG and the diagonalization of the correlation matrix w.r.t. $\mathbf{T}' \otimes \mathbf{R}$ rather than \mathbf{T} and \mathbf{R} separately. This leads, as we show next, to the equations of the type

$$\mathbf{T}' \otimes \mathbf{R} = \mathbf{X}. \quad (10)$$

Hence, in the following, whenever we use *jointly optimized* we mean it in the sense of finding an optimal solution to the matrix equation of the type of (10), where \mathbf{R} and \mathbf{T} are the unknowns. This problem belongs to the nearest Kronecker product (NKP) problems family, which are generally only solved approximately by applying both linear and nonlinear optimization methods [24]. For the sake of completeness we give a description of a method in Section . In the same section we provide exact solutions for the case when \mathcal{R}_m has a Kronecker structure.

Propositions 1, 2 and 3 summarize the main results of this section.

Proposition 1: Assume the multimode field realizations of the channel \mathbf{m} are known. Then the maximum MEG of a MIMO antenna

system comprising a N_r -port receive antenna and a N_t -port transmit antenna is given by G_{ei} , which upper bounds MEG, i.e.,

$$G_e \leq G_{ei} = 16\pi^2 \sum_{i=1}^{N_r} \eta_i \sum_{j=1}^{N_t} \eta_j, \quad (11)$$

where G_{ei} is achieved for the jointly link-matched transmission and reception coefficients, i.e., conjugate mode matching

$$(\mathbf{T}' \otimes \mathbf{R})_{n,t} = c_n m_t^*, \quad (12)$$

where $()^*$ denotes complex-conjugate and

$$\sum_n |c_n|^2 = \frac{16\pi^2 \sum_{i=1}^{N_r} \eta_i \sum_{j=1}^{N_t} \eta_j}{\|\mathbf{m}\|^2}, \quad (13)$$

where η_i and η_j are the radiation efficiencies of ports i and j of the receive and transmit antennas, respectively, and φ_n is an arbitrary phase factor.

The derivation is given in Appendix A.

Proposition 1 is an extension to the MIMO case of a similar result presented in [16] for a multi-element antenna system deployed only at one end of the communications link.

The physical interpretation is that the MIMO link power is maximized when all channel multimodes are jointly conjugate-matched by the receive and the transmit antennas. This would require the knowledge of each realization of the \mathbf{M} -matrix, which can be deemed unpractical for rapidly varying channels. However, if the channel is constant over fairly long periods of time, then the channel could, in principle, be estimated. Another important observation is that (12) allows fixing the transmit antenna coefficients and then finding the optimum receive antenna coefficients and viceversa, i.e., if the antenna coefficients of one end of the communications link are required to be fixed by some design constraints then we can find the optimum coefficients of the other end such that the average link power/MEG is maximized.

Proposition 2: Assume the correlation matrix of the multimode field realizations of the channel \mathcal{R}_m is given. Then the maximum MEG of a MIMO antenna system comprising a N_r -port receive antenna and a N_t -port transmit antenna is given by G_{ea} , which upper bounds MEG, i.e.,

$$G_e \leq G_{ea} = 16\pi^2 \sum_{i=1}^{N_r} \eta_i \sum_{j=1}^{N_t} \eta_j \frac{\lambda_{\{max\}}}{\text{tr}\{\mathcal{R}_m\}}, \quad (14)$$

where G_{ea} is achieved by the largest eigenvalue λ_{\max} of the eigenvalue problem

$$\mathbf{X}\mathcal{R}_m - \lambda\mathbf{X} = 0, \quad (15)$$

where

$$\mathbf{X} = \mathbf{T}' \otimes \mathbf{R}, \quad (16)$$

Hence, the optimal value is achieved jointly for the transmission and reception coefficients.

See Appendix B for a derivation.

3.2. MIMO Correlation Minimization

In the previous section we provided the conditions that maximize the MIMO average link power. In this section we instead study the diagonalization of the MIMO full-correlation matrix.

Proposition 3: The full-correlation matrix \mathcal{R}_h of a MIMO system consisting of a N_r -port receive antenna and a N_t -port transmit antenna in a random multimode field with correlation matrix \mathcal{R}_m is diagonalized as

$$\mathcal{R}_h = 16\pi^2 \sum_{i=1}^{N_r} \eta_i \sum_{j=1}^{N_t} \eta_j \Lambda_{m,M_s}, \quad (17)$$

by the jointly optimized transmission and reception coefficients

$$\mathbf{T}' \otimes \mathbf{R} = 4\pi e^{i\varphi} \sqrt{\frac{\sum_{i=1}^{N_r} \eta_i \sum_{j=1}^{N_t} \eta_j}{M_s}} \mathbf{U}_{m,M_s}^\dagger, \quad (18)$$

where Λ_{m,M_s} is diagonal matrix containing the M_s strongest and distinct eigenvalues of \mathcal{R}_m , and $\mathbf{U}_{m,M_s}^\dagger$ is the matrix containing the corresponding eigenvectors.

The derivation is given in Appendix C.

The physical interpretation of Proposition 3 is that in order to diagonalize the correlation matrix of the MIMO channel and at the same time to obtain the largest possible link power then the columns of the matrix $\mathbf{T}' \otimes \mathbf{R}$ should be chosen so that they equal the eigenvectors of the matrix \mathcal{R}_m corresponding its M_s strongest and distinct eigenvalues. Hence, the receiver and transmitter must be jointly optimized to achieve channel diagonalization in average.

Remark 1: The link MEG corresponding to the minimum correlation involving a N_r -port receive antenna and a N_t -port transmit

antenna in a random multimode field with correlation matrix \mathcal{R}_m is

$$G_{ed} = 16\pi^2 \sum_{i=1}^{N_r} \eta_i \sum_{j=1}^{N_t} \eta_j \frac{\text{tr}\{\Lambda_{m,M_s}\}}{M_s \text{tr}\{\mathcal{R}_m\}}, \quad (19)$$

which describes the MIMO average link power between the outgoing (output) signal from the receive antenna port i and the signals incoming (input) signals at the transmit antenna port j .

The derivation is straightforward and therefore omitted.

It is worthwhile to notice that (19) does not correspond to an optimized MEG value since the criterion has been the diagonalization of the correlation matrix. Furthermore, we see that G_{ei} , G_{ea} and G_{ed} satisfy the following inequalities.

Corollary 1: Given that the number of receive N_r and transmit N_t antenna ports are fixed, then the link MEG between two multi-element antenna systems satisfies the following inequalities

$$G_{ed} \leq G_{ea} \leq G_{ei}, \quad (20)$$

where G_{ed} , G_{ea} and G_{ei} are given by (19), (14) and (11), respectively. Equality is achieved if \mathcal{R}_m is a rank-one matrix or, equivalently, if $\lambda_{\max} = \text{tr}\{\mathcal{R}_m\}$.

This result follows directly from Propositions 1, 2 and 3. Indeed, the first inequality follows directly by noticing that $M_s \lambda_{\max} \geq \text{tr}\{\Lambda_{m,M_s}\}$, while the second inequality is obtained by observing that $\sum \lambda_n = \text{tr}\{\mathcal{R}_m\}$, where λ_n are the distinct eigenvalues of the hermitian matrix \mathcal{R}_m . The equality conditions follow straightforwardly.

4. THE NEAREST KRONECKER PRODUCT (NKP) PROBLEM

As we have shown above, the joint optimization of transmit and receive antenna coefficients involves solving equations of the type (10). A general solution of this type of problem is not known. However, a solution is obtained by recasting this problem as a nearest Kronecker product (NKP) problem [24], which we present in Subsection 4.1. We then in Subsection 4.2, under the assumption of the Kronecker model for the MIMO full-correlation matrix, provide exact solutions to the posed NKP problems.

4.1. Approximate Solution to a Constrained NKP Problem

Assume that $\mathbf{T} \in \mathbb{C}^{M_t \times N_t}$, $\mathbf{R} \in \mathbb{C}^{N_r \times M_r}$ and $\mathbf{X} \in \mathbb{C}^{N_t N_r \times M_t M_r}$, then a solution is obtained by solving the minimum least square problem

$$\begin{aligned} \min & \|\mathbf{X} - \mathbf{T}' \otimes \mathbf{R}\|_F^2 \\ \text{s.t. } & \text{tr}\{\mathbf{T}\mathbf{T}^\dagger\} = 4\pi \sum_{i=1}^{N_t} \eta_i, \quad \text{tr}\{\mathbf{R}^\dagger \mathbf{R}\} = 4\pi \sum_{j=1}^{N_r} \eta_j. \end{aligned} \quad (21)$$

This minimization problem can be rewritten [24] as

$$\begin{aligned} \min & \|\mathfrak{R}(\mathbf{X}) - \text{vec}(\mathbf{T}') \text{vec}'(\mathbf{R})\|_F^2 \\ \text{s.t. } & \text{tr}\{\mathbf{T}\mathbf{T}^\dagger\} = 4\pi \sum_{i=1}^{N_t} \eta_i, \quad \text{tr}\{\mathbf{R}^\dagger \mathbf{R}\} = 4\pi \sum_{j=1}^{N_r} \eta_j, \end{aligned} \quad (22)$$

where $\mathfrak{R}(\mathbf{X})$ is the rearrangement function given below

$$\mathfrak{R}(\mathbf{X}) = \begin{bmatrix} \text{vec}'(\mathbf{X}^{11}) \\ \vdots \\ \text{vec}'(\mathbf{X}^{N_t 1}) \\ \vdots \\ \text{vec}'(\mathbf{X}^{1 M_t}) \\ \vdots \\ \text{vec}'(\mathbf{X}^{N_t M_t}) \end{bmatrix}, \quad (23)$$

where \mathbf{X}^{kl} is the (k, l) -th $N_r \times M_r$ block of \mathbf{X} . The rearrangement has the property

$$\mathfrak{R}(\mathbf{T}' \otimes \mathbf{R}) = \text{vec}(\mathbf{T}') \text{vec}'(\mathbf{R}). \quad (24)$$

The minimization problem (22) is a rank-one approximation problem and has a straightforward solution involving the SVD [24], i.e., if

$$\mathfrak{R}(\mathbf{X}) = \mathbf{U}\mathbf{\Sigma}\mathbf{V}^\dagger, \quad (25)$$

is the SVD of $\mathfrak{R}(\mathbf{X})$, then the optimum \mathbf{T} and \mathbf{R} are given by

$$\text{vec}(\mathbf{T}') = \sqrt{4\pi \sum_{i=1}^{N_t} \eta_i} \mathbf{U}(:, 1), \quad (26)$$

and

$$\text{vec}(\mathbf{R}) = \sqrt{4\pi \sum_{j=1}^{N_r} \eta_j} \mathbf{V}^*(:, 1), \quad (27)$$

where $\mathbf{U}(:, 1)$ and $\mathbf{V}(:, 1)$ are the singular vector corresponding to the largest singular value in (25). The derivation is similar to the unconstrained NKP problem and therefore omitted; see [24] for further reference.

Hence, (26) and (27) represent an approximate solution to (10) with which help we can compute the corresponding far-field radiation pattern, (4) and (5). It is however desirable to obtain exact solutions. This is not always possible, but under some assumptions, i.e., the Kronecker correlation channel, an exact solution can be found. This is discussed next.

4.2. An Exact Solution to the Constrained NKP Problem under the Assumption of a Kronecker Correlation Matrix

In this section we specialize the full-correlation matrix (9) to the Kronecker multimode correlation channel model, i.e.,

$$\mathcal{R}_m = \mathcal{R}'_{M_t} \otimes \mathcal{R}_{M_r}, \quad (28)$$

where

$$\mathcal{R}_{M_r} = \langle \mathbf{M}\mathbf{M}^\dagger \rangle \quad \text{and} \quad \mathcal{R}_{M_t} = \langle \mathbf{M}^\dagger \mathbf{M} \rangle, \quad (29)$$

are the multimode channel correlation matrices at the receiver and the transmitter, respectively. We now see that under this assumptions inserting (28) into (8) and applying the property of Kronecker products $(\mathbf{A} \otimes \mathbf{B})(\mathbf{C} \otimes \mathbf{D}) = \mathbf{A}\mathbf{C} \otimes \mathbf{B}\mathbf{D}$ we obtain the Kronecker product model for the MIMO channel too

$$\mathcal{R}_h = \mathcal{R}'_{H_t} \otimes \mathcal{R}_{H_r}, \quad (30)$$

where

$$\mathcal{R}_{H_r} = \mathbf{R}\mathcal{R}_{M_r}\mathbf{R}^\dagger \quad \text{and} \quad \mathcal{R}_{H_t} = \mathbf{T}^\dagger \mathcal{R}_{M_t} \mathbf{T}. \quad (31)$$

The applicability of model (30) to real propagation channels has been proved limited [25]. However, under some special conditions it can still be a good working model, e.g., when the correlation statistics at one end of the link is determined by a local scattering process and is less sensitive to changes at the other end of the link [26, 27].

Based on the above model we state the following propositions.

Proposition 4: Assume the correlation matrix of the multimode field realizations of the channel \mathcal{R}_m admits the Kronecker decomposition (28). Then, the optimal receive and transmit antenna coefficients that maximize the link power/MEG (7) are given by

$$\mathbf{R} = \mathbf{J}_{M_r}^{11} \mathbf{U}_{M_r}^\dagger \quad \text{and} \quad \mathbf{T} = \mathbf{U}_{M_t} \mathbf{J}_{M_t}^{11}, \quad (32)$$

where $\mathbf{J}_{M_r}^{11}$ and $\mathbf{J}_{M_t}^{11}$ are single-entry matrices, where element (1, 1) equals one and the rest equal zero. Matrices \mathbf{U}_{M_r} and \mathbf{U}_{M_t} are unitary matrices satisfying

$$\mathcal{R}_{M_r} = \mathbf{U}_{M_r} \Sigma_{M_r} \mathbf{U}_{M_r}^\dagger \quad \text{and} \quad \mathcal{R}_{M_t} = \mathbf{U}_{M_t} \Sigma_{M_t} \mathbf{U}_{M_t}^\dagger. \quad (33)$$

The derivation is provided in Appendix D.

It now becomes clear that (32) and (33) are the solution to the NKP problem (21) under the assumption (15), (16) and (28).

The physical interpretation of Proposition 4 is that in a MIMO Kronecker channel, the optimum receive antenna is a single-port antenna exciting different modes, while the optimum transmit antenna is a multi-port antenna, where each port excites only one mode. Hence, in a Kronecker channel, the optimal antenna system in the sense of Proposition 2 is a MISO system instead of a MIMO system. However, multiple-element antennas are required at both link ends to achieve the maximum in both the up- and the down-link.

Proposition 5: The full-correlation matrix \mathcal{R}_h of a MIMO system consisting of a N_r -port receive antenna and a N_t -port transmit antenna in a random multimode field with correlation matrix \mathcal{R}_m that admits the Kronecker decomposition (28) is diagonalized by receive and transmit antenna coefficients given by

$$\mathbf{R} = \mathbf{U}_{M_r}^\dagger \quad \text{and} \quad \mathbf{T} = \mathbf{U}_{M_t}, \quad (34)$$

where \mathbf{U}_{M_r} and \mathbf{U}_{M_t} unitary satisfy (33), i.e., the matrices containing the eigenvectors of \mathcal{R}_{M_r} and \mathcal{R}_{M_t} , respectively.

The derivation is given in Appendix E. As a result of Proposition 5 we have here that (34) and (33) are the solution to the NKP problem (21) under the assumption (18) and (28). The physical interpretation is straightforward.

5. NUMERICAL EXAMPLES

In this section we illustrate, by means of numerical examples, some of the results derived above. We focus on MIMO antenna coefficients satisfying one of the three cases:

- (i) Proposition 1, i.e., maximum MEG based on knowledge of the multimode channel realization.
- (ii) Proposition 4, i.e., maximum MEG based on the multimode correlation matrix. The provided solution is exact under the Kronecker model assumption.
- (iii) Proposition 5, i.e., minimum correlation through multimode correlation matrix diagonalization. The provided solution is exact under the Kronecker model assumption.

For the sake of simplicity we aim at studying antennas exciting the three lowest TM modes, i.e., the three electrical dipole modes.

We use a simple channel model based on the more advanced channel models presented in [28, 29] (For justifications of the different assumptions in this model, see [16]). The models for the AoA (angle-of-arrival) and the AoD (angle-of-departure) for each of the two orthogonal polarizations assume a two-dimensional Laplacian distribution in spherical coordinates, i.e.,

$$\begin{aligned} p_{\theta, \phi x}(\theta, \phi) &= p_{\theta x}(\theta)p_{\phi x}(\phi) \\ &= Ae^{-(\sqrt{2}|\theta-\mu_{\theta}|/\sigma_{\theta}+\sqrt{2}|\phi-\mu_{\phi}|/\sigma_{\phi})} \sin \theta, \end{aligned} \quad (35)$$

where the elevation angle $\theta \in [0, \pi]$, azimuth angle $\phi \in [0, 2\pi]$ and x stands for either of $\hat{\theta}$ - or $\hat{\phi}$ -polarization, and the shape is controlled by the distribution parameters $\{\mu_{\theta x}, \sigma_{\theta x}, \mu_{\phi x}, \sigma_{\phi x}\}$. We further assume that $\sigma = \sigma_{\theta x} = \sigma_{\phi x} = 0.1$ rad at the receive antenna, while at the transmit antenna $\sigma = \sigma_{\theta x} = \sigma_{\phi x} = 10$ rad emulating channels of small and large angle spread, respectively. We further assume that $\mu_{\theta x} = \pi/2$, $\mu_{\phi x} = 0$ rad at both the transmit and the receive antennas. The cross-polarization ratio, XPR, of the channel is assumed to be equal 6 dB. XPR is defined as the ratio of the power of the vertically polarized waves to the power of horizontally polarized waves [22].

We can now obtain the multimode expansion coefficients \mathbf{M} of the MIMO channel matrix \mathbf{H} defined by the Kronecker channel model (28) and (29). Figure 2 illustrates the absolute value of the corresponding multimode correlation matrices at the transmitter and the receiver and the multimode full-correlation matrix in plots (a), (c) and (b), respectively. As we can see Figure 2(a), the spatial selectivity resulting from a low angle spread at the transmitter also leads to a distinct selectivity in the multimode domain. This, in addition to

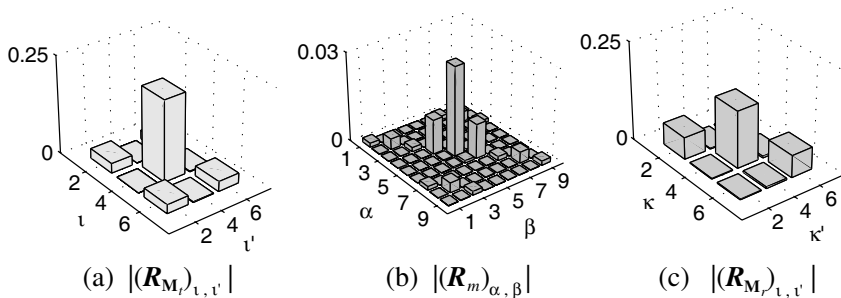


Figure 2. Absolute value of (a) the multimode correlation matrices at the transmitter, (c) at the receiver and (b) the multimode full-correlation matrix.

the prevalence of the vertically polarized channel component over the horizontally polarized channel component (determined by the XPR), results in the TM mode with multi-index $\iota = 2$, i.e., $\tau = 2, l = 1, m = 0$ having the higher power as compared to the other two TM dipole modes. At the receiver side we see a slightly similar behavior; however, here the channel is “more diagonal” due to the large angle spread which leads to uncorrelated modes. Also here, the power of the TM mode with multi-index $\iota = 2$ is slightly larger than the two other modes due to the large XPR value.

Figure 3 shows the absolute value of the transmit and receive antenna coefficients obtained by the optimization criteria defined above. Indeed, Figures 3(a) and (d) correspond to antennas satisfying criterium (i) (the solution is only approximate), Figures 3(b) and (e) correspond to antennas satisfying criterium (ii), which is an exact solution and finally, Figures 3(c) and (f) correspond to antennas satisfying criterium (iii), which is also an exact solution. The obtained antenna coefficients depend on the propagation channel parameters in our example. Obviously, a different channel model will naturally also lead to different values of antenna coefficients. However, the resulting MIMO full-correlation matrix between antenna elements should be diagonal independently of the channel model for each specific

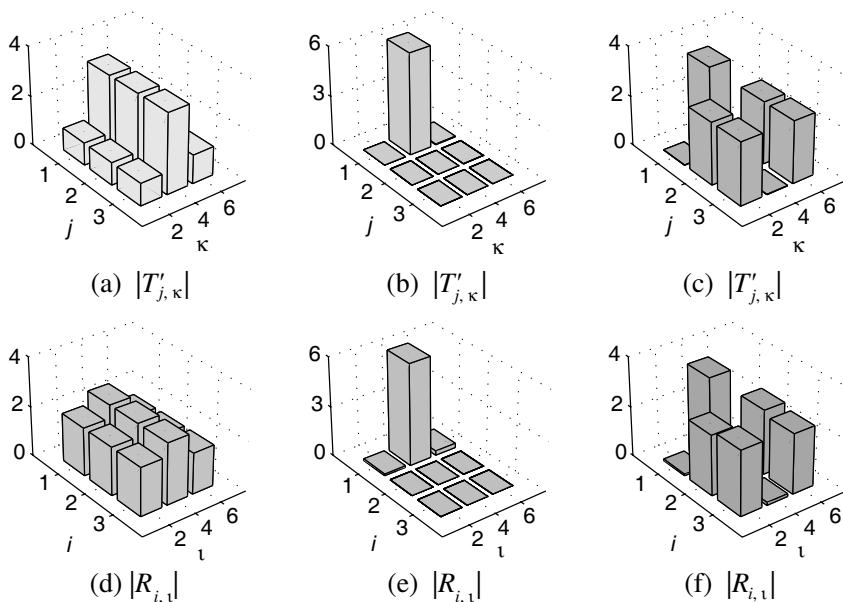


Figure 3. Absolute value of the transmit and receive antenna coefficients (i.e., \mathbf{T} and \mathbf{R}) obtained by different optimization criteria.

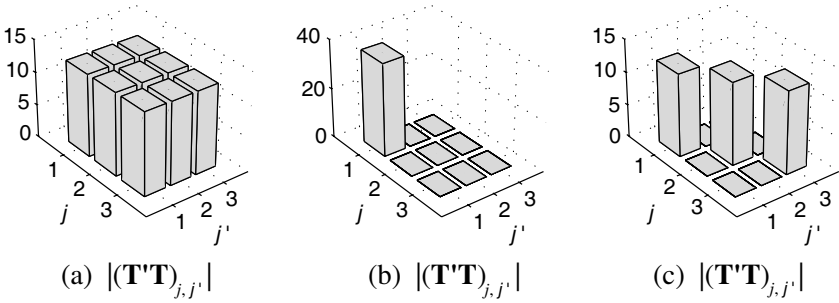


Figure 4. Absolute value of the correlation between transmit antenna elements shown in Figure 3.

criterion. Figure 4 shows absolute value of the correlation matrix corresponding to the three illustrated criteria. Figure 4(a) shows that maximizing MEG based on the channel realization results in fully-correlated antennas, which in turn result in fully correlated MIMO links as shown in Figure 5(a). Figure 4(b) shows that maximizing MEG based on the multimode correlation matrix results in the power being concentrated on one antenna, which leads to almost a single link being excited as depicted in Figure 5(b). Figure 4(c) shows that uncorrelated antenna elements in the sense Proposition 5 also lead to uncorrelated MIMO channels as shown in Figure 5(c). The MEG, or rather $G_e/4\pi N_r N_t$, corresponding to the analyzed cases are, -0.6 dB for case (i), -3.4 dB for case (ii) and -9.5 dB for case (iii), where we have taken into account that $N_r = 1$ in case (ii) while $N_r = 3$ in the other two cases. As we can see, MEG considered in these cases also satisfy inequalities (20) since in our specific example $N_r = M_s = 3$ for cases (ii) and (iii). We can now see that, in Kronecker channels, the first inequality in (20) is satisfied if $M_s/N_r > \text{tr}\{\Lambda_{m,M_s}\}/\lambda_{\max}$.

It is worthwhile to notice that a closer analysis of Figure 5(c) corroborates the fact that antennas exploiting polarization diversity may, in general, result in unbalanced antenna branches. Indeed, although the optimized antenna patterns are orthogonal (see Figure 4(c)) as well as the corresponding MIMO channel links, the average link power is not balanced among the links. This is also due to the low angle spread at the transmitter side. Hence, to require uncorrelated MIMO links is not the best strategy in this case. Instead, as well-known, beamforming would be a much better approach to exploit the correlation of the channel. For a channel with XPR equal 0 dB, i.e., equal power in the vertical and horizontal polarizations, the MIMO link power would had been more balanced. Furthermore, if the angle spread is large at both the transmitter and the receiver the optimized antennas would provide a diagonal correlation matrix with

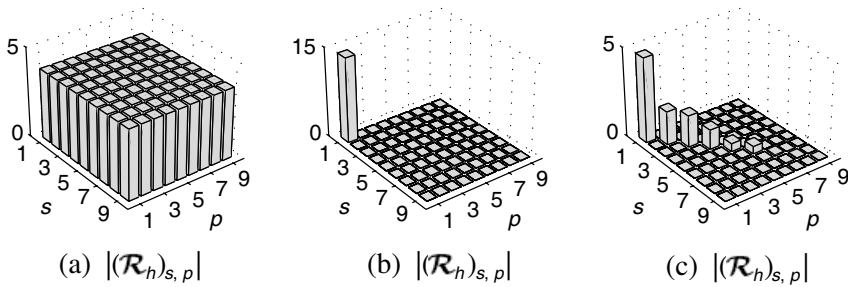


Figure 5. Absolute value of the MIMO full-correlation matrix.

elements of equal magnitudes, i.e., links with identical power.

As predicted in Chu's seminal work [30], the radiation properties of an antenna are related to its size. Moreover, the size of the antenna poses limits to the magnitude of svw modes. Indeed, although we have limited our analysis to consider only dipole modes, wireless devices usually may excite higher order modes too. However, the contribution of higher order modes will be attenuated (filtered out, see, e.g., [31]), because of the high losses associated with large l . In [32] Chus's antenna gain limitations have been extended to antenna pattern limitations that take into account the propagation channel modes. These results are of practical relevance to antenna design and measurements of wireless devices operating in multipath environments [33–36], and requiring both a good bandwidth and power efficiency.

6. CONCLUSIONS

We have provided optimality conditions for MIMO antenna coefficients in wireless channels. The analysis has been focused on the Mean Effective Gain (MEG) and the full-correlation matrix of the MIMO link between multi-element antennas operating in a multipath channel. Based on a spherical vector wave multimode expansion coefficients of the MIMO channel matrix we provide a definition of the link MEG in this case. We show that searching for optimal antenna coefficients leads to a Near Kronecker Product (NKP) problem formulation both when the optimization is based on the realization of multimode channel coefficients or their correlation matrix. Although a general solution to this problem does not exist, we find exact solutions under the special assumption of the Kronecker model for the correlation matrix. These results are of great practical importance to the development of new advanced antenna designs and over-the-air testing of MIMO wireless devices.

ACKNOWLEDGMENT

This work has been partly supported by the EU FP6 ‘‘GAWIND’’ project and the EU FP7 IAPP ‘‘IAPP@RANPLAN’’ project.

APPENDIX A. PROOF OF PROPOSITION 1

We can apply the Cauchy-Schwartz-Buniakovskii inequality to (6) to get

$$\begin{aligned} \|\mathbf{h}\|^2 &= \|(\mathbf{T}' \otimes \mathbf{R}) \mathbf{m}\|^2 = \sum_n \left| \sum_\iota (\mathbf{T}' \otimes \mathbf{R})_{n,\iota} m_\iota \right|^2 \\ &\leq \sum_n \sum_\iota \left| (\mathbf{T}' \otimes \mathbf{R})_{n,\iota} \right|^2 \|\mathbf{M}_\iota\|^2. \end{aligned} \quad (\text{A1})$$

Observing that

$$\begin{aligned} \sum_n \sum_\iota \left| (\mathbf{T}' \otimes \mathbf{R})_{n,\iota} \right|^2 &= \text{tr} \left\{ (\mathbf{T}' \otimes \mathbf{R})^\dagger (\mathbf{T}' \otimes \mathbf{R}) \right\} \\ &= \text{tr} \left\{ \mathbf{T} \mathbf{T}^\dagger \otimes \mathbf{R}^\dagger \mathbf{R} \right\} = \text{tr} \left\{ \mathbf{T} \mathbf{T}^\dagger \right\} \text{tr} \left\{ \mathbf{R}^\dagger \mathbf{R} \right\}, \end{aligned} \quad (\text{A2})$$

we arrive at the following inequality

$$\|\mathbf{h}\|^2 \leq \|\mathbf{m}\|^2 \text{tr} \left\{ \mathbf{T} \mathbf{T}^\dagger \right\} \text{tr} \left\{ \mathbf{R}^\dagger \mathbf{R} \right\}. \quad (\text{A3})$$

Equality is achieved when

$$(\mathbf{T}' \otimes \mathbf{R})_{n,\iota} = c_n m_\iota^*, \quad (\text{A4})$$

where c_n is a complex constant. Using the Lorentz condition for reciprocal antennas (5) and by applying the following normalization

$$|v_i|^2 = 1, \quad (\text{A5})$$

and

$$\frac{1}{2\eta k^2} \int \mathbf{F}_i(\hat{\mathbf{r}}) \cdot \mathbf{F}_i^*(\hat{\mathbf{r}}) d\Omega = 4\pi\eta_i, \quad (\text{A6})$$

we get for the transmission coefficients for either the receiver or the transmit antenna

$$\sum_\iota |T_{\iota,i}|^2 = 4\pi\eta_i. \quad (\text{A7})$$

Hence, the constants c_n satisfy the normalization

$$\sum_n |c_n|^2 = \frac{16\pi^2 \sum_{i=1}^{N_r} \eta_i \sum_{j=1}^{N_t} \eta_j}{\|\mathbf{m}\|^2}. \quad (\text{A8})$$

Then, we finally arrive at the inequality that concludes the derivation

$$\|\mathbf{h}\|^2 \leq 16\pi^2 \sum_{i=1}^{N_r} \eta_i \sum_{j=1}^{N_t} \eta_j \|\mathbf{m}\|^2. \quad (\text{A9})$$

APPENDIX B. PROOF OF PROPOSITION 2

From (7) we see that if the multimode expansion coefficients of the MIMO channel are not known, but instead we know their correlation matrix then we need to solve the optimization problem

$$\begin{aligned} & \max \operatorname{tr} \{ \mathbf{T}' \otimes \mathbf{R} \} \mathcal{R}_m (\mathbf{T}' \otimes \mathbf{R})^\dagger \\ & \text{s.t. } \operatorname{tr} \left\{ (\mathbf{T}' \otimes \mathbf{R}) (\mathbf{T}' \otimes \mathbf{R})^\dagger \right\} = 16\pi^2 \sum_{i=1}^{N_r} \eta_i \sum_{j=1}^{N_t} \eta_j. \end{aligned} \quad (\text{B1})$$

Now denoting $\mathbf{X} = \mathbf{T}' \otimes \mathbf{R}$ we can solve (B1) by the Lagrange multiplier method, which in this particular case has the known solution (15), where we have used the identity $\frac{\partial \operatorname{tr}(\mathbf{X}\mathbf{A}\mathbf{X}^\dagger)}{\partial \mathbf{X}} = \mathbf{X}^* \mathbf{A}^t$ for $\mathbf{X} \in \mathbb{C}$ and $\mathbf{A} \in \mathbb{C}$.

APPENDIX C. PROOF OF PROPOSITION 3

Given the correlation matrix for the link elements

$$\mathcal{R}_h = (\mathbf{T}' \otimes \mathbf{R}) \mathcal{R}_m (\mathbf{T}' \otimes \mathbf{R})^\dagger, \quad (\text{C1})$$

perform the diagonalization $\mathcal{R}_m = \mathbf{U}\Lambda_m\mathbf{U}^\dagger$, which gives

$$\mathcal{R}_h = (\mathbf{T}' \otimes \mathbf{R}) \mathbf{U}\Lambda_m\mathbf{U}^\dagger (\mathbf{T}' \otimes \mathbf{R})^\dagger, \quad (\text{C2})$$

where $\mathbf{U}^{\infty \times \infty}$ is a unitary matrix and $\Lambda_m^{\infty \times \infty}$ a diagonal matrix. Now choose $\mathbf{T}' \otimes \mathbf{R} = c\mathbf{U}_{m,M_s}^\dagger$, where \mathbf{U}_m is a matrix containing M_s first eigenvectors of \mathbf{U} , corresponding the ordered eigenvalues in Λ_{m,M_s}

$$\mathcal{R}_h = |c|^2 \mathbf{U}_{m,M_s}^\dagger \mathbf{U}\Lambda_m\mathbf{U}^\dagger \mathbf{U}_{m,M_s} = |c|^2 \Lambda_{m,M_s}. \quad (\text{C3})$$

Now, using the normalization of the transmit and receive coefficients in (21)–(22) and observing that

$$(\mathbf{T}' \otimes \mathbf{R}) (\mathbf{T}' \otimes \mathbf{R})^\dagger = |c|^2 \mathbf{U}_{m,M_s}^\dagger \mathbf{U}_{m,M_s} = |c|^2 \mathbf{I}_{M_s \times C}, \quad (\text{C4})$$

and

$$\operatorname{tr} \left\{ (\mathbf{T}' \otimes \mathbf{R}) (\mathbf{T}' \otimes \mathbf{R})^\dagger \right\} = 16\pi^2 \sum_{i=1}^{N_r} \eta_i \sum_{j=1}^{N_t} \eta_j = |c|^2 M_s, \quad (\text{C5})$$

we arrive to the final result (17).

APPENDIX D. PROOF OF PROPOSITION 4

Inserting (28) and (16) into (15) gives

$$(\mathbf{T}' \otimes \mathbf{R}) (\mathcal{R}'_{\mathbf{M}_t} \otimes \mathcal{R}_{\mathbf{M}_r}) - \lambda (\mathbf{T}' \otimes \mathbf{R}) = 0. \quad (\text{D1})$$

Now inserting (33) into (D1) and regrouping using the property of Kronecker products $(\mathbf{A} \otimes \mathbf{B})(\mathbf{C} \otimes \mathbf{D}) = \mathbf{AC} \otimes \mathbf{BD}$ we obtain

$$(\mathbf{T}' \otimes \mathbf{R}) (\mathbf{U}_{\mathbf{M}_t}^* \otimes \mathbf{U}_{\mathbf{M}_r}) \Sigma_{\mathbf{M}} (\mathbf{U}_{\mathbf{M}_t}^* \otimes \mathbf{U}_{\mathbf{M}_r})^\dagger - \lambda (\mathbf{T}' \otimes \mathbf{R}) = 0, \quad (\text{D2})$$

where

$$\Sigma_{\mathbf{M}} = \Sigma_{\mathbf{M}_t} \otimes \Sigma_{\mathbf{M}_r}. \quad (\text{D3})$$

We now readily see that since we seek a solution corresponding to the largest eigenvalue then \mathbf{R} and \mathbf{T} should satisfy the following condition

$$(\mathbf{T}' \otimes \mathbf{R}) (\mathbf{U}_{\mathbf{M}_t}^* \otimes \mathbf{U}_{\mathbf{M}_r}) = \mathbf{J}_{\mathbf{M}}^{11}, \quad (\text{D4})$$

where $\mathbf{J}_{\mathbf{M}}^{11}$ is a single-entry matrices, where element $(1, 1)$ is one and the rest are zero. From this we obtain (32), which concludes our derivation.

APPENDIX E. PROOF OF PROPOSITION 5

Inserting (28) into (8) gives

$$\mathcal{R}_{\mathbf{h}} = (\mathbf{T}' \otimes \mathbf{R}) (\mathcal{R}'_{\mathbf{M}_t} \otimes \mathcal{R}_{\mathbf{M}_r}) (\mathbf{T}' \otimes \mathbf{R})^\dagger. \quad (\text{E1})$$

Now inserting (33) into (E1) and regrouping using the property of Kronecker products $(\mathbf{A} \otimes \mathbf{B})(\mathbf{C} \otimes \mathbf{D}) = \mathbf{AC} \otimes \mathbf{BD}$ we obtain

$$\mathcal{R}_{\mathbf{h}} = (\mathbf{T}' \mathbf{U}_{\mathbf{M}_t}^*) \otimes (\mathbf{R} \mathbf{U}_{\mathbf{M}_r}) \Sigma_{\mathbf{M}} (\mathbf{T}' \mathbf{U}_{\mathbf{M}_t}^*)^\dagger \otimes (\mathbf{R} \mathbf{U}_{\mathbf{M}_r})^\dagger. \quad (\text{E2})$$

Now, since we are seeking to diagonalize $\mathcal{R}_{\mathbf{h}}$, then (34) must be satisfied.

REFERENCES

1. Winters, J. H., "On the capacity of radio communications systems with diversity in Rayleigh fading environments," *IEEE Journal on Selected Areas in Communications*, Vol. 5, 871–878, Jun. 1987.
2. Telatar, I. E., "Capacity of multi-antenna Gaussian channels," *European Transactions on Telecommunications*, Vol. 10, Nov.–Dec. 1999.
3. Foschini, G. J., "Layered space-time architecture for wireless communication in a fading environment when using multi-element antennas," *Bell Labs Tech. J.*, Vol. 1, 41–59, 1996.

4. Tulino, A., A. Lozano, and S. Verdu, "Impact of antenna correlation on the capacity of multi-antenna channels," *IEEE Transactions on Information Theory*, Vol. 51, 2491–2509, Jul. 2005.
5. Suvikunnas, P., J. Villanen, K. Sulonen, C. Icheln, J. Ollikainen, and P. Vainikainen, "Evaluation of the performance of multi-antenna terminals using a new approach," *IEEE Transactions on Instrumentation and Measurement*, Vol. 55, 1804–1813, Oct. 2006.
6. 3GPP-Technical Specification Group Radio Access Network, "Measurement of radiated performance for MIMO and multi-antenna reception for HSPA and LTE terminals," Tech. Rep. 3GPP TR 37.976 V1.1.0, 3GPP and 3GPP2; download at <http://www.3gpp.org>, 06 2010 (Release 10).
7. Jakes, W. C. and D. Cox, *Microwave Mobile Communications*, IEEE Press, 1994.
8. Vaughan, R. and J. Bach Andersen, *Channels, Propagation and Antennas for Mobile Communications*, Institution of Electrical Engineers, 2003.
9. Wallace, J. and M. Jensen, "Mutual coupling in MIMO wireless systems: A rigorous network theory analysis," *IEEE Transactions on Wireless Communications*, Vol. 3, 1317–1325, Jul. 2004.
10. Wallace, J. and M. Jensen, "Termination-dependent diversity performance of coupled antennas: Network theory analysis," *IEEE Transactions on Antennas and Propagation*, Vol. 52, 98–105, Jan. 2004.
11. Andersen, J. B. and B. K. Lau, "On closely coupled dipoles in a random field," *IEEE Antennas and Wireless Propagation Letters*, Vol. 5, No. 1, 73–75, Dec. 2006.
12. Lau, B. K., J. B. Andersen, G. Kristensson, and A. F. Molisch, "Impact of matching network on bandwidth of compact antenna arrays," *IEEE Transactions on Antennas and Propagation*, Vol. 54, 3225–3238, Nov. 2006.
13. Migliore, M. D., "On the role of the number of degrees of freedom of the field in MIMO channels," *IEEE Transactions on Antennas and Propagation*, Vol. 54, No. 2, 620–628, 2006.
14. Hanlen, L. and M. Fu, "Wireless communication systems with-spatial diversity: A volumetric model," *IEEE Transactions on Wireless Communications*, Vol. 5, 133–142, Jan. 2006.
15. Jensen, M. and J. Wallace, "Capacity of the continuous-space electromagnetic channel," *IEEE Transactions on Antennas and Propagation*, Vol. 56, 524–531, Feb. 2008.

16. Alayon Glazunov, A., M. Gustafsson, A. F. Molisch, F. Tufvesson, and G. Kristensson, "Spherical vector wave expansion of Gaussian electromagnetic fields for antenna-channel interaction analysis," *IEEE Transactions on Antennas and Propagation*, Vol. 57, 2055–2067, Jul. 2009.
17. Alayon Glazunov, A., M. Gustafsson, A. Molisch, and F. Tufvesson, "Physical modelling of multiple-input multiple-output antennas and channels by means of the spherical vector wave expansion," *IET Microwaves, Antennas & Propagation*, Vol. 4, 778–791, Jun. 2010.
18. Alayon Glazunov, A., "On the antenna-channel interactions: A spherical vector wave expansion approach," Doctoral Thesis, ISSN 1654-790X, No. 16, Electrical and Information Technology, Mar. 2009.
19. Hansen, J. E., ed., *Spherical Near-field Antenna Measurements*, Peter Peregrinus, London, UK, 1988.
20. Hansen, W. W., "A new type of expansion in radiating problems," *Phys. Review*, Vol. 47, 139–143, Jan. 1935.
21. Brock, B. C., "Using vector spherical harmonics to compute antenna mutual impedance from measured or computed fields," Unlimited Release SAND2000-2217-Revised, SANDIA REPORT, Sandia National Laboratories Albuquerque, New Mexico 87185 and Livermore, California 94550, Apr. 2001.
22. Taga, T., "Analysis for mean effective gain of mobile antennas in land mobile radio environments," *IEEE Transactions on Vehicular Technology*, Vol. 39, 117–131, May 1990.
23. Alayon Glazunov, A., A. Molisch, and F. Tufvesson, "Mean effective gain of antennas in a wireless channel," *IET Microwaves, Antennas & Propagation*, Vol. 3, 214–227, Mar. 2009.
24. Loan, C. F. V. and N. Pitsianis, *Linear Algebra for Large Scale and Real Time Applications*, Approximations with Kronecker products, 293–314, Kluwer Academic Publishers, 1993.
25. Wyne, S., A. F. Molisch, P. Almers, G. Eriksson, J. Karedal, and F. Tufvesson, "Outdoor-to-indoor office MIMO measurements and analysis at 5.2 GHz," *IEEE Transactions on Vehicular Technology*, Vol. 57, 1374–1386, May 2008.
26. Kermoal, J. P., L. Schumacher, K. I. Pedersen, P. E. Mogensen, and F. Frederiksen, "A stochastic MIMO radio channel model with experimental validation," *IEEE Journal on Selected Areas in Communications*, Vol. 20, 1211–1226, Aug. 2002.

27. Sivasondhivat, K., J.-I. Takada, I. Ida, and Y. Oishi, "Polarimetric Kronecker separability of site-specific double-directional channel in an urban macrocellular environment," *EURASIP Journal on Wireless Communications and Networking*, Vol. 2009, 2009.
28. Correia, L. (ed.), *COST 259 Final Report: Wireless Flexible Personalised Communications*, Wiley, 2001.
29. Correia, L. (ed.), *COST 273 Final Report: Towards Mobile Broadband Multimedia Networks*, Elsevier, 2006.
30. Chu, L. J., "Physical limitations of omni-directional antennas," *Appl. Phys.*, Vol. 19, 1163–1175, 1948.
31. Hiegler, T., A. Friederich, F. M. Landstorfer, and G. Fässler, "Efficient antenna performance measurement system for gsm handsets by use of a near-field to far-field transformation algorithm," *IEE Technical Seminar on Antenna Measurements and SAR*, 28–29, Burleigh Court, Loughborough University, UK, 2002.
32. Glazunov, A., M. Gustafsson, and A. Molisch, "On the physical limitations of the interaction of a spherical aperture and a random field," *IEEE Transactions on Antennas and Propagation*, Vol. 59, 119–128, Jan. 2011.
33. Khatun, A., T. Laitinen, and P. Vainikainen, "Spherical wave modelling of radio channels using linear scanners," *2010 Proceedings of the Fourth European Conference on Antennas and Propagation (EuCAP)*, 1–5, Apr. 2010.
34. Evans, D. N. and M. A. Jensen, "Near-optimal radiation patterns for antenna diversity," *IEEE Transactions on Antennas and Propagation*, 2010.
35. Mohajer, M., S. Safavi-Naeini, and S. K. Chaudhuri, "Spherical vector wave method for analysis and design of MIMO antenna systems," *IEEE Antennas and Wireless Propagation Letters*, Vol. 9, 1267–1270, 2010.
36. Alayon Glazunov, A. and J. Zhang, "Some examples of uncorrelated antenna radiation patterns for MIMO applications," *PIERS Proceedings*, 598–602, Marrakesh, Morocco, Mar. 20–23, 2011.